ARMY RESEARCH LABORATORY

Multidimensional, Two-Phase Simulations of Notional Telescoped Ammunition Propelling Charge

by Michael J. Nusca, Albert W. Horst, and James F. Newill

ARL-TR-3306   **September 2004**

NOTICES

Disclaimers

The findings in this report are not to be construed as an official Department of the Army position unless so designated by other authorized documents.

Citation of manufacturer's or trade names does not constitute an official endorsement or approval of the use thereof.

Destroy this report when it is no longer needed. Do not return it to the originator.

Army Research Laboratory

Aberdeen Proving Ground, MD 21005-5066

Multidimensional, Two-Phase Simulations of Notional Telescoped Ammunition Propelling Charge

Michael J. Nusca, Albert W. Horst, and James F. Newill
Weapons and Materials Research Directorate, ARL

REPORT DOCUMENTATION PAGE

1. REPORT DATE (DD-MM-YYYY)	2. REPORT TYPE	3. DATES COVERED (From - To)
September 2004	Final	April 2003–April 2004

4. TITLE AND SUBTITLE	5a. CONTRACT NUMBER
Multidimensional, Two-Phase Simulations of Notional Telescoped Ammunition Propelling Charge	
	5b. GRANT NUMBER
	5c. PROGRAM ELEMENT NUMBER
6. AUTHOR(S)	5d. PROJECT NUMBER
Michael J. Nusca, Albert W. Horst, and James F. Newill	622618H8000
	5e. TASK NUMBER
	5f. WORK UNIT NUMBER

7. PERFORMING ORGANIZATION NAME(S) AND ADDRESS(ES)	8. PERFORMING ORGANIZATION REPORT NUMBER
U.S. Army Research Laboratory ATTN: AMSRD-ARL-WM-BD Aberdeen Proving Ground, MD 21005-5066	ARL-TR-3306

9. SPONSORING/MONITORING AGENCY NAME(S) AND ADDRESS(ES)	10. SPONSOR/MONITOR'S ACRONYM(S)
	11. SPONSOR/MONITOR'S REPORT NUMBER(S)

12. DISTRIBUTION/AVAILABILITY STATEMENT

Approved for public release; distribution is unlimited.

13. SUPPLEMENTARY NOTES

14. ABSTRACT

One of the many challenges facing weapon developers is the requirement for a highly lethal, lightweight, and compact large-caliber gun system. One concept recently investigated by the U.S. Army is that of a swing-chamber gun, necessitating the use of telescoped ammunition. Such ammunition not only reduces the volume available for the propellant change, but also places severe geometric constraints on both the distribution of the propellant and the location and functionality of the ignition system. Lumped parameter codes cannot capture the influence of these configurational complexities on the processes of flamespreading and the formation of ensuing pressure waves. One-dimensional, two-phase flow interior ballistic simulations reveal the likelihood of such waves and raise the concern for possible damage to the ammunition (projectile). Multidimensional, two-phase interior ballistic simulations provide quantitative predictions of the flow in the annular region between the sidewall of the telescoped projectile and the cartridge case, also show the formation of pressure waves, and further the concern over projectile damage. Initial results are shown from ongoing work to couple an interior ballistics code with a gun/projectile structural dynamics code. Pressure waves in the charge produce a very demanding environment for the projectile which necessitates the use of a more substantial structure, with the attending sharp reduction in cargo capacity, or the use of exotic materials in order to insure a successful launch.

15. SUBJECT TERMS

gun charges, solid propellant, multiphase flow, computer simulation

16. SECURITY CLASSIFICATION OF:			17. LIMITATION OF ABSTRACT	18. NUMBER OF PAGES	19a. NAME OF RESPONSIBLE PERSON
a. REPORT	b. ABSTRACT	c. THIS PAGE			Michael J. Nusca
UNCLASSIFIED	UNCLASSIFIED	UNCLASSIFIED	UL	24	19b. TELEPHONE NUMBER (Include area code) 410-278-6108

Contents

List of Figures

1. Introduction

As described in our previous reports on this subject (*1, 2*), the fundamental problem of increasing gun interior ballistic performance is one of increasing the area under the pressure travel curve without exceeding maximum pressure limits of the system. The classic approach to solving this problem involves two key components: first, one must increase the total amount of chemical energy in the propellant charge; and second, one must control its release such that the maximum desirable chamber pressure is reached as soon as possible and maintained as long as possible until burnout occurs. The former is traditionally addressed through the development and use of higher energy propellant formulations and propellant geometries that facilitate higher loading densities. The latter is pursued by configuring the propellant geometry such that an ever-increasing burning surface is presented as a function of burn distance and/or providing a change in propellant chemistry to increase rate as a function of burn distance.

However, this is simply the macroscopic, or system level, description of the problem. In truth, this competition between gas production and volume production is not simply one of global concern, but rather extremely important on the local level, as either a nonuniform initial distribution of propellant in the gun chamber or a localized ignition of the propellant bed can lead to significant longitudinal pressure waves with attendant safety problems, the process being further influenced by grain configuration and loading density, which determine overall charge permeability to gas flow, and propellant mechanical properties, which determine the potential for grain fracture (*1*). Consider the generic, large-caliber, high-performance telescoped round of figure 1 and one might easily imagine the presence of most if not all of the above-named exacerbating features.
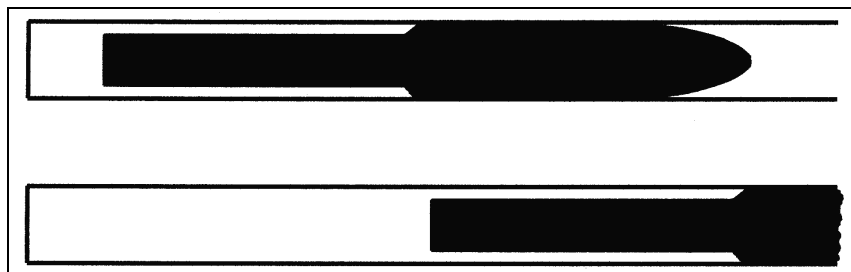
Figure 1. Initial projectile/chamber interfaces at time of ignition of main propelling charge for untranslated and translated cargo projectile (notional) (*1*).

The previously referenced paper (*1*) provided both lumped-parameter and one-dimensional (with area change), two-phase flow representations of such a configuration. In particular, we presented calculations performed for a notional 18-kg projectile of the submunition-carrying cargo type, fired from a nominal 105-mm gun at a maximum chamber pressure of 330 MPa using JA2

propellant at a maximum loading density of 0.95 g/cm³. The round was assumed to be telescoped, that is, the projectile initially loaded such that it seats far back into the case for compact size and automated handling and loading. The firings were assumed to take place with the projectile either initially in its original telescoped position, or translated, with the projectile moved forward out of the case before ignition of the main charge. These two conditions are depicted in figure 1.

Calculations performed using a standard lumped parameter interior ballistic code (*3*) yielded muzzle velocity predictions of 809 and 778 m/s for the untranslated and translated rounds respectively, the reduction in muzzle velocity for the initially translated round accruing from the larger initial chamber volume allowing less expansion of the combustion gases working on the base of the projectile and the reduction in the overall projectile travel over which acceleration can take place. Predicted breech and projectile base pressure vs. time curves are shown in figure 2, necessarily smooth owing to the assumptions of the lumped parameter analysis but revealing slight differences in shape depending on initial projectile position.
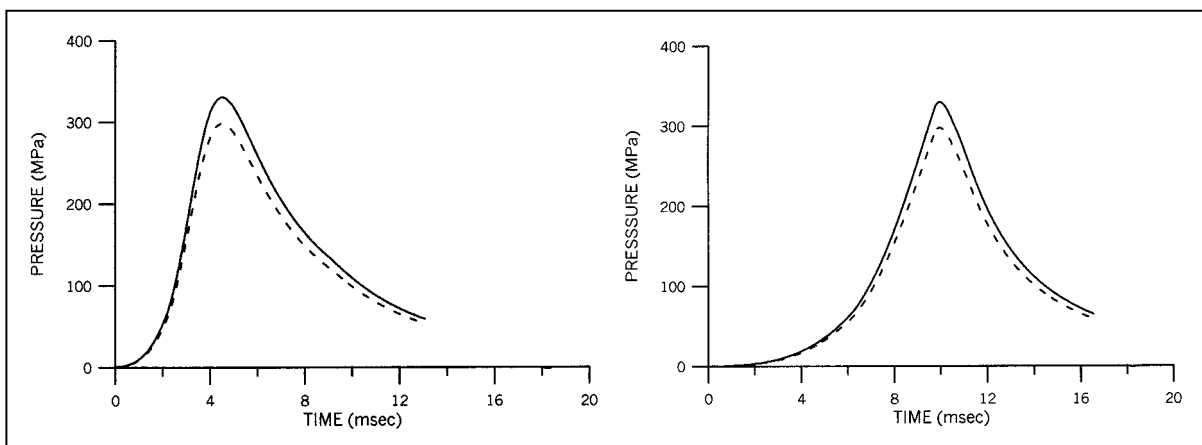
Figure 2. Predicted (IBHVG2) breech (solid) and projective base (dashed) pressure-vs.-time curves for untranslated (left) and translated (right) projectile (notional) (*1*).

From a performance standpoint, it appears that the untranslated round offers a significant advantage; moreover, the lack of a requirement for translation of the projectile prior to motion of the main charge is clearly desirable. However, the lumped parameter treatment is unaware of any of such configurational issues and their possible impact on the formation of pressure waves—motivating the application of more rigorous modeling approaches. Toward that end, the previous study then employed the XKTC code (*4*), a two-phase flow interior ballistic code capable of addressing the macroscopic features of the longitudinal flow and resulting pressure field, subject to a one-dimensional (with area change) representation. Figure 3 reveals the first of a series of calculations performed in that study, revealing substantial pressure waves apparently associated with the change in cross-sectional area and flow in the narrow annular region external to the telescoped portion of the projectile—in this case, for a round conservatively configured to have no propellant initially loaded in this annular region.
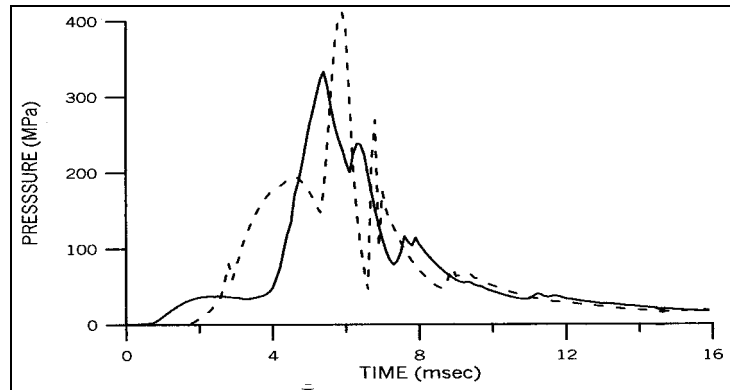
Figure 3. Predicted (XKTC) pressure-vs.-time curves
(breech—solid; projectile base—dashed) for
untranslated projectile—no propellant in annulus (*1*).

Concerns raised by this and subsequent related calculations were only heightened by the
development of experimental data for a related configuration, subsequently evaluated under the
Army's Multi-Role Armament and Ammunition System (MRAAS) Program (*1*, *2*, *5*).

2.   Description of the NGEN Code

The Army's NGEN3 code is a multidimensional, multiphase CFD code that incorporates
three-dimensional continuum equations along with auxiliary relations into a modular code
structure (*6*, *7*). Because accurate charge modeling involves flowfield components of both a
continuous and a discrete nature, a coupled Eulerian-Lagrangian approach is used. On a
sufficiently small scale of resolution in both space and time, the components of the flow are
represented by the balance equations for a multicomponent reacting mixture describing the
conservation of mass, momentum, and energy. A macroscopic representation of the flow is
adopted using these equations derived by a formal averaging technique applied to the
microscopic flow. These equations require a number of constitutive laws for closure including
state equations, intergranular stresses, and interphase transfer. The numerical representation of
these equations, as well as the numerical solution thereof, is based on a finite-volume
discretization and high-order accurate, conservative numerical solution schemes. The spatial
values of the dependent variables at each time step are determined by a numerical integration
method, denoted the Continuum Flow Solver (CFS), which treats the continuous phase and
certain of the discrete phases in an Eulerian fashion. The Flux-Corrected Transport scheme (*8*) is
a suitable basis for the CFS because the method is explicit and has been shown to adapt easily to
massively parallel computer systems. The discrete phases are treated by a Lagrangian
formulation, denoted the Large Particle Integrator (LPI), which tracks the particles explicitly and
smoothes discontinuities associated with boundaries between propellants yielding a continuous

3

distribution of porosity over the entire domain. The manner of coupling between the CFS and the LPI is through the attribution of properties (e.g., porosity and mass generation) at points in the flow. The size of the grid as well as the number of Lagrangian particles is user prescribed.

For the simulations of novel solid propellant configurations, such as disks stacked axially along the chamber centerline and/or thin annular concentric layers (wraps), the NGEN code takes a macroscopic approach (*9–13*). These solid propellant media are modeled using Lagrange particles that regress, produce combustion product gases, and respond to gasdynamic and physical forces. Individual grains, sticks, slab, and wrap layers are not resolved; rather, each medium is distributed within a specified region in the gun chamber. The constitutive laws that describe interphase drag, form-function, etc., assigned to these various media, determine preferred gas flow paths through the media and responses of the media to forces. Media regions can be encased in impermeable boundaries that yield to gasdynamic flow after a prescribed pressure load is reached. Details of the NGEN code are supplied elsewhere (*6, 7*).

3. Description of the Nominal (Degenerate) Problem

Owing to the developing nature of the NGEN code, just described, as well as the lack of certainty about the actual configuration of any large-caliber telescoped ammunition that may be pursued in the future, a simplified propelling charge/chamber interface was defined for this study. Presented in figure 4, we note the features of a large afterbody intrusion of the projectile into the region normally occupied by propellant has been preserved, but that any configurational complexities associated with tapers or steps have been eliminated. Further, we note that we have exaggerated the extent of the annular region by diminishing the diameter of the projectile afterbody which facilitates examination of various features of the propelling charge in this region. The chamber is untapered and of 14-cm diameter and 84-cm length. The main charge is assumed to be 7-perforated JA2 granular propellant, loaded in two regions—one axial (region III) and one annular (region IV) each with a loading density of 0.9 g/cm^3 (i.e., the loading limit for granular propellant). See figure 4 for dimensions of these regions. Ignition of these main propellant regions, in all cases, is provided by two small regions of propellant materials that are mounted along the breechface—25 g of ignited M1 propellant (region I) and 25 g of black powder at ambient initial temperature (region II). The projectile mass is 18, 144 g (40 lb). Three pressure taps are located along the chamber wall (denoted R, M, and F).
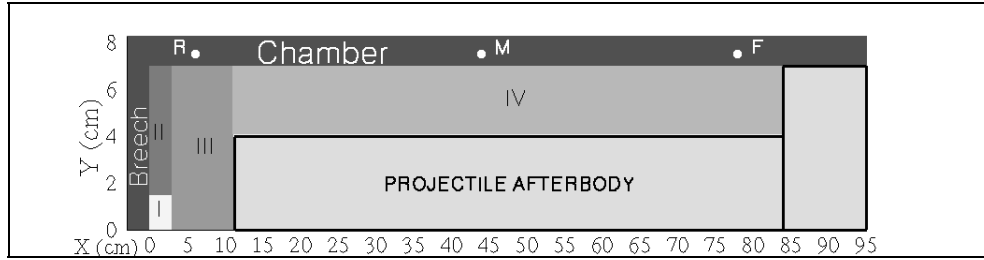
4

Figure 4. Axisymmetric representation of notional (degenerate) problem—chamber, projectile afterbody, and four propellant regions shown; note that region IV fills the annular volume.

4.   Results and Discussion

The first simulation involves both the rear and annular regions in the gun chamber filled with propellant at the stated loading density (figure 4). A prediction using the NGEN code of the resulting pressure-vs.-time curves at three locations along the chamber wall (i.e., 6, 43, and 78 cm from the breech face) is provided in figure 5. These results essentially duplicate the gross features of the severe longitudinal pressure waves, though not in all details, of the experimental data (*1*, *2*, *5*) and also correspond to the prediction using the XKTC code (figure 3). This not-unexpected result follows from the base ignition of a tightly packed bed of granular propellant, the situation being exacerbated as the convectively driven combustion front and accompanying pressure rise passes into the region of the much smaller cross-sectional area in the annular region external to the intruding projectile. While not unexpected, it is reassuring that a similarity of behavior is predicted by both a 1-D and a 2-D interior ballistics code for this largely 1-D (with area change) propelling charge configuration.

The flamespreading process of this first notional charge can be described, however, in greater detail using the NGEN code, as demonstrated by the sequence of pressure fields depicting the development and evolution of pressure waves in the chamber (figure 6). This series of computed pressure contours is shown in gray-scale from 0.1 to 350 MPa and above (i.e., white to dark black) along with overplotted gray contours lines. Velocity vectors (shown in black) are overlaid so as to depict both the direction and magnitude of gases in the chamber. For each time, the chamber and projectile afterbody is shown from the common centerline to the radial wall of the chamber. The locations of the three pressure collection points, used in figure 5, are also shown along the chamber wall for reference. During the time sequence displayed in figure 6, flow within the propellant loaded into the rear region is highly 2-D, while the flow within the annular propellant region is largely 1-D. The formation, reflection, and damping of pressure waves in the annular region can be clearly seen up to the time of significant projectile movement (2.6 ms) and peak pressurization of the breech (3.0 ms). Although space does not permit the display of
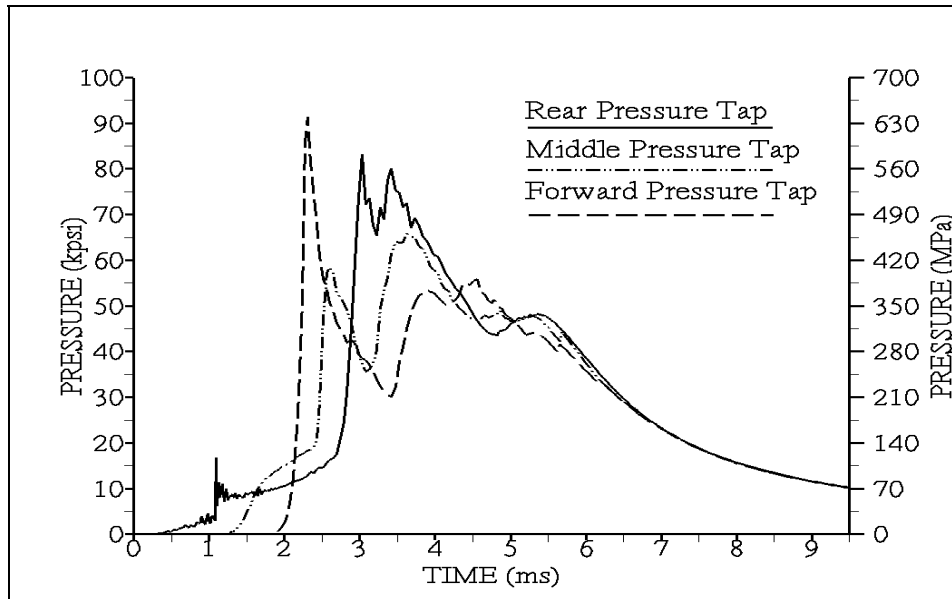
5

Figure 5. Pressure-vs.-time curves predicted using the NGEN code for both the rear and annular propellant regions fully filled—results for three locations along the chamber wall.

propellant porosity contours, these computed results clearly show the formation of a propellant bed material compression wave that tracks with the pressure waves described previously and shown in figure 6.

Past studies have identified the importance of persistent annular regions external to bagged artillery charges in mitigating strong longitudinal pressure waves when the failure of the centercore igniter led to a base ignition (*14*, *15*). Application of this principle to the present study lead to calculations performed on a configuration which separated the annular region in our test configuration into an inner annulus (i.e., along the projectile afterbody) filled with propellant (region IV) and an adjacent outer empty annulus, as shown in figure 7. Computed pressure-vs.-time curves (figure 8) as well as the simulation of the evolution of pressure fields (figure 9) confirms once again the importance of this high-permeability path in reducing the severity of longitudinal pressure waves. Unfortunately, in addition to reducing pressure waves, the reduction in overall propellant load also reduces performance, the maximum pressure dropping from 525 to 150 MPa, and projectile muzzle velocity from 1470 to 1185 m/s.

Evidently, a desirable feature of the charge loaded in the annular region would be the use of a propellant that allows a high loading density but with a low interphase drag (i.e., low resistance to flow) in the axial direction. This is clearly not a new result in general, but rather one that apparently takes on even more importance in configurationally complex charge configurations involving significant reductions in cross-sectional flow area. As a limiting-case numerical experiment, a calculation was then performed involving the annular region filled with propellant (see figure 4), as in the case leading to the results for figures 5 and 6, but this time with the
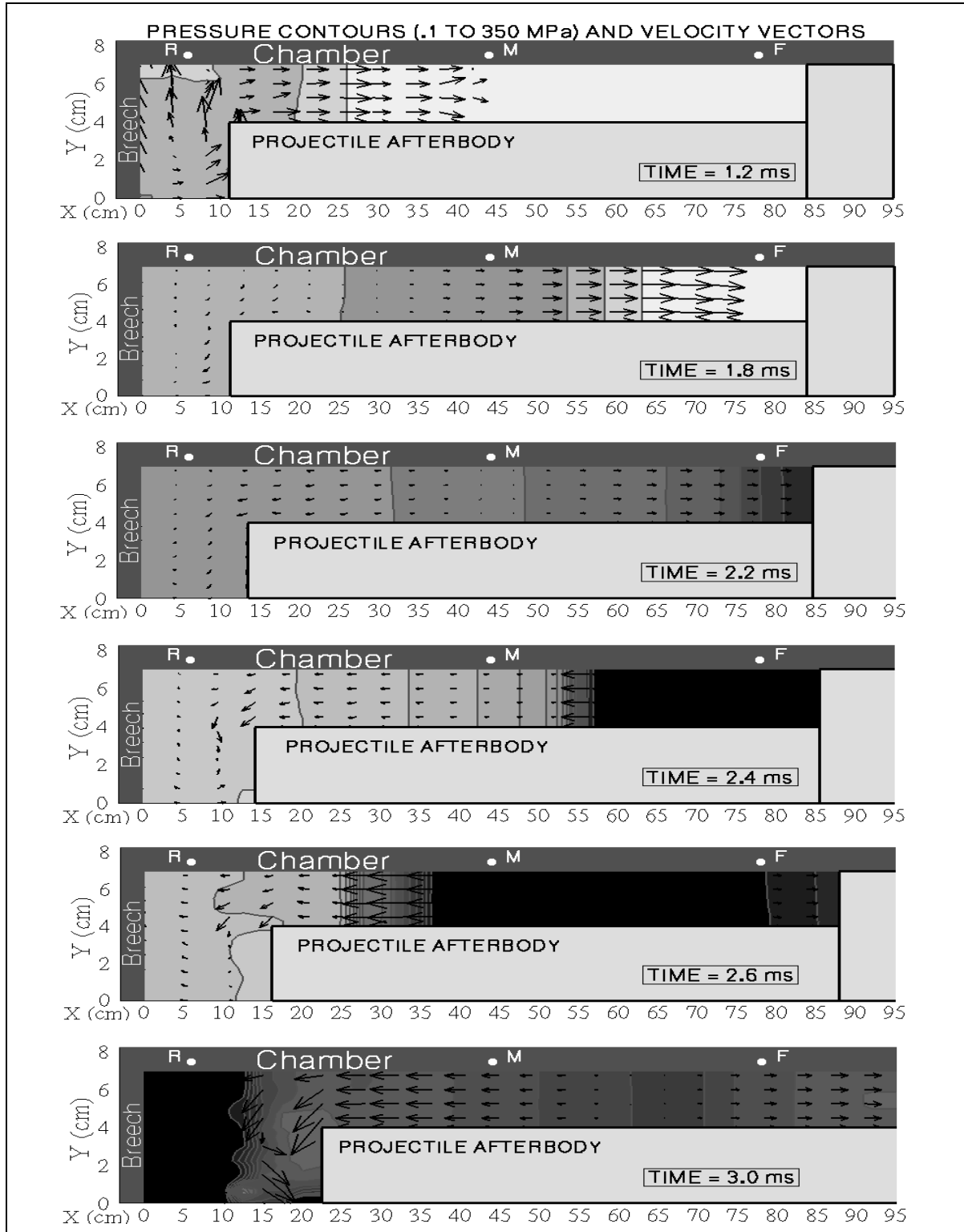
6

Figure 6. Gas pressure contours and velocity vectors within the chamber fully filled with propellant (see figure 4) as predicted using the NGEN code—results shown in gray-scale (white to black: 0.1–350 MPa).
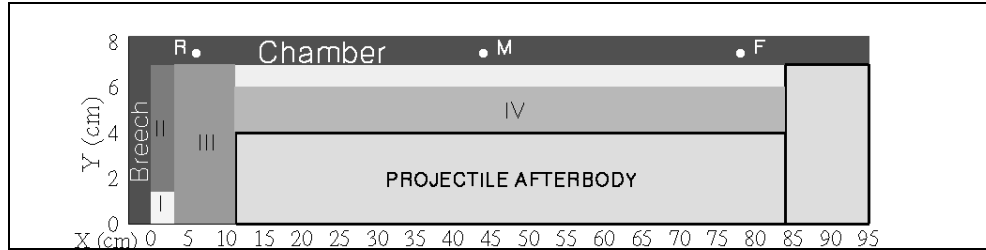
Figure 7. Axisymmetric representation of second notional (degenerate) problem—chamber,
projectile afterbody, radial ullage, four propellant regions shown; note region IV
does not fill the annular volume.
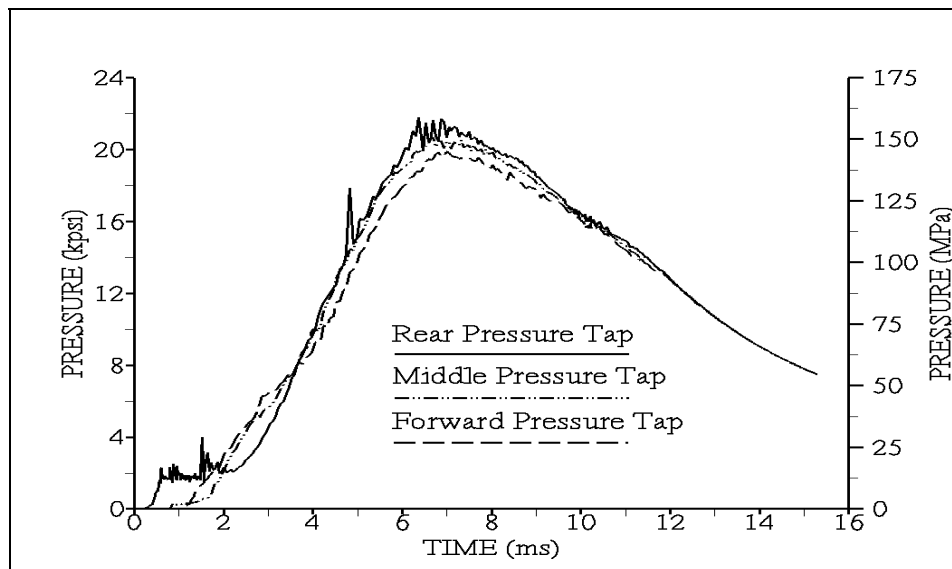
Figure 8. Pressure-vs.-time curves predicted using the NGEN code for the rear
propellant region fully filled and the annular propellant region partially
filled—results for three locations along the chamber wall.

interphase drag in region IV eliminated. The resulting pressure-vs.-time curves, presented in
figure 10a, confirm the desired result, substantially reducing the magnitude of longitudinal
pressure waves—this time, without a significant loss in performance (i.e., muzzle velocity of
1350 m/s). As a practical alternative, the propellant in region IV could be replaced by multiple
layers of thin (0.35-cm) propellant wrapped concentrically around the projectile afterbody. Such
an arrangement fills the region between the projectile and the chamber wall but allows natural
flow paths in the axial direction. The resulting pressure-vs.-time curves, presented in figure 10b,
confirm the desired result, reducing the magnitude of longitudinal pressure waves and
maintaining a muzzle velocity of 1400 m/s. While such results have long been understood for
conventional ammunition configurations, its effectiveness in telescoped configurations has been
shown for the first time, we believe, in an earlier paper (2) and further explored in the present
results.

8

Figure 9. Gas pressure contours and velocity vectors within the chamber partially filled with propellant (see figure 7) as predicted using the NGEN code—results shown in gray-scale (white to black: 0.1–120 MPa).
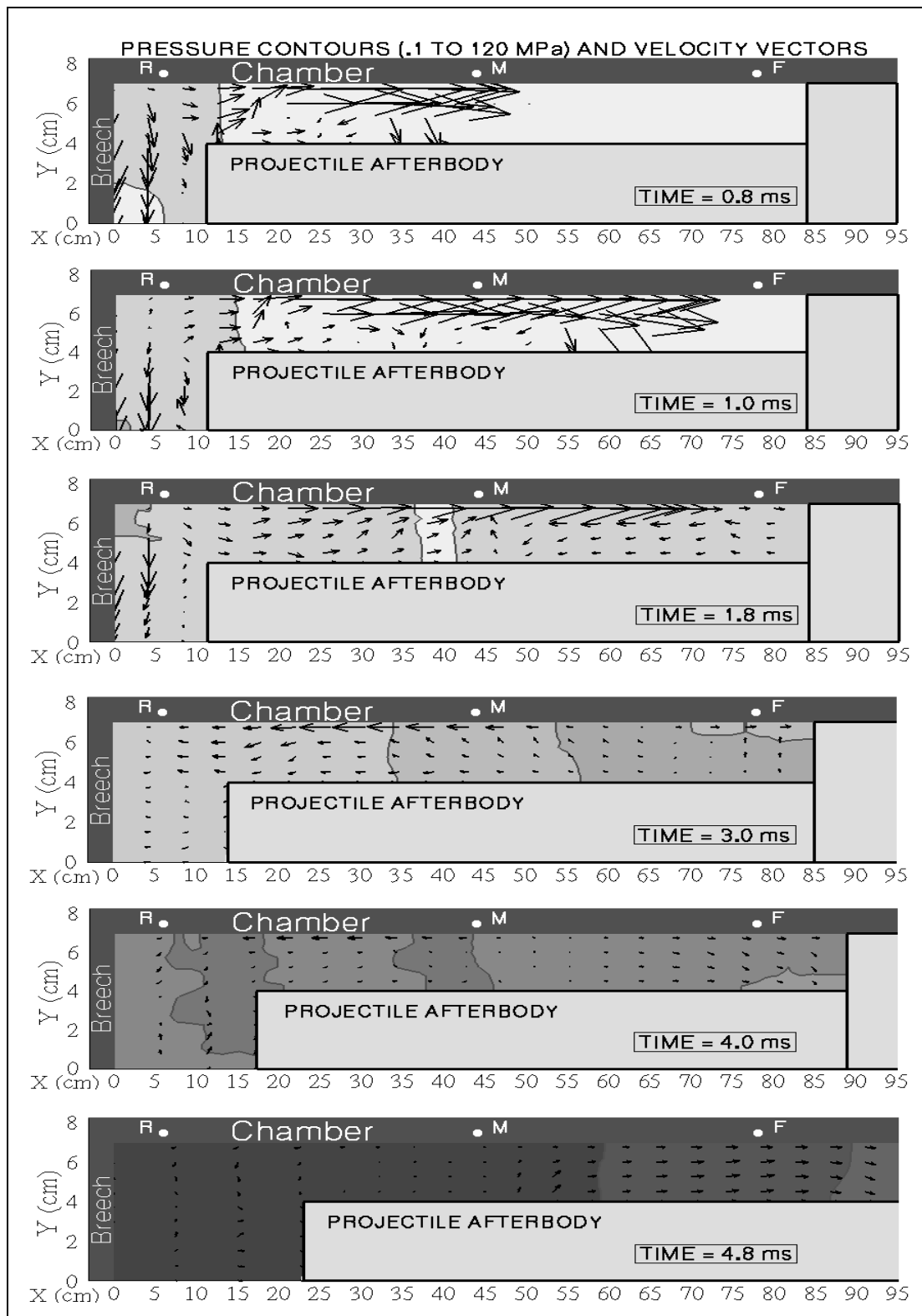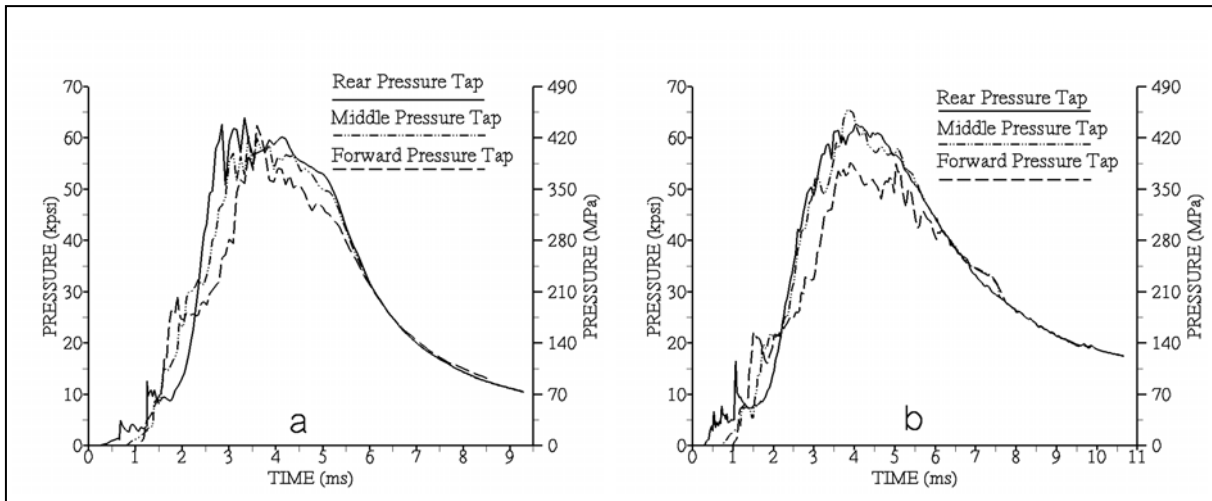
9

Figure 10. Pressure-vs.-time curves predicted using the NGEN code for the annular region (region IV figure 4) filled with propellant of (a) grains with null interphase drag and (b) concentric wrap.

5. Simulation of the Projectile Structural Response

Figures 5 and 6 show a pressure field that is challenging for the designer of the projectile structure. In order to assess the implication of pressure waves generated by the propelling charge on the projectile structure, or possibly proposing a structure that may withstand the pressure oscillations when these waves cannot be remedied, the material response of the projectile to these waves must be obtained. Gun/projectile structural simulations have been used by the U.S. Army Research Laboratory (ARL) to assess the dynamic response of cannon launched projectiles since the late 1980s (*16*). These gun/projectile dynamics codes are actually a suite of software tools used to construct and update material models for dynamic simulations. In recent years, this software suite has been modified in order to allow coupled simulations, i.e., a programmed interaction between computational fluid dynamics (CFD) codes for interior ballistics, such as XKTC (*4*) and NGEN (*7*), and computational structural mechanics (CSM) codes. While this suite of software is necessary for model development, data reduction, and visualization, the solution of the CSM problems are primarily done through Lawrence Livermore National Laboratory's DYNA3D code (*17*).

Because the computational domain of the NGEN code accounts solely for the portion of the projectile immersed in the propellant change (recall figure 4), a forebody for the notional projectile used in this study was created. This front for the projectile was created to yield a wheelbase similar to that recently tested for 120-mm projectiles, while also providing for maximum cargo capacity. The notional projectile contacts the bore through two bourrelets spaced 178 mm (7 in) (see figure 11). While this configuration may not precisely represent
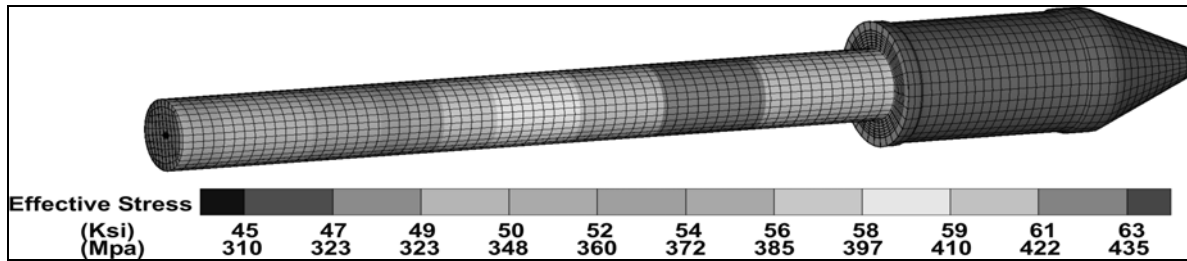
10

Figure 11. Pressures on the projectile afterbody at 4 ms; predicted using the NGEN code and transferred to the DYNA structural dynamics code.

ammunition configurations of interest, it is similar to several current projectile concepts and provides insight into issues resulting from projectiles that intrude into the charge. In these CSM simulations, the response of a projectile payload was ignored. It should be noted that coupling between the NGEN interior ballistics code and the DYNA3D materials/structures code is solely single path, i.e., computed projectile surface deformations, if any, are not accounted for in the NGEN simulations. The relaxation of this assumption which would yield full coupling of CFD and CSM codes is beyond the scope of the current work but is the subject of ongoing research in CFD-CSM.

Figure 11 shows the projectile considered in this study with an afterbody identical to that shown in figure 4 and with the notional forebody created for the CSM simulation. The "effective stress" shown in this figure is actually the wall pressure computed using the NGEN code (as shown in figures 5 and 6) and entered into the DYNA3D code's database. Although the NGEN simulation spans the time from charge initiation to projectile muzzle exit, a single time frame is shown in the figure. Note that the peak pressure load does not occur near the extremes of the projectile afterbody, rather the peak pressure occurs ~25% of afterbody length behind the location of engagement (sealing) on the gun tube.

The material stresses resulting from this pressure loading is complex. Figure 12 shows the computed effective stress for a projectile made from aluminum (7075 T6 with an ~552-MPa [80-ksi] yield and an ~621-MPa [90-ksi] failure), assuming a 12.7-mm (0.5-in) wall thickness. As shown in the figure, stresses in the projectile have, even at this early time, exceeded material failure strength over half of the afterbody indicating an almost certain material failure as the projectile travels inbore.
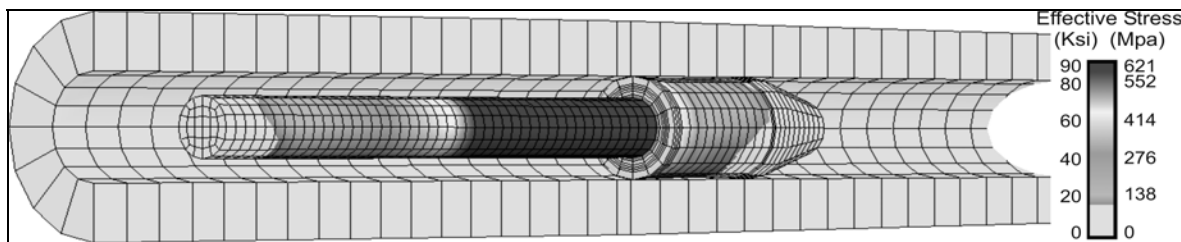

Figure 12. Effective stress as predicted using the DYNA code, for an aluminum projectile with 12.7-mm (0.5-in) wall thickness at 2.4 ms.

11

This CSM calculation demonstrates that, while maintaining reasonable cargo space (i.e., relatively thin wall projectile afterbody) with contemporary materials (e.g., aluminum), a typical projectile afterbody design will not withstand the pressure environment in the gun chamber while immersed in the propellant charge as described in figures 4–6.

In order to further this illustration, the projectile material was changed to steel. Figure 13a shows the computed stress vs. time for three locations on the afterbody that is now composed of a 12.7-mm (0.5-in) steel wall. Again, the projectile wall pressures during the interior ballistics cycle were computed using the NGEN code (as shown in figures 5 and 6) and input to the DYNA3D code (as shown in figure 12). Note the "double peak" in the stress (figure 13a) that is similar to the pressure history shown in figure 5. This highly time-dependent pressure and thus stress behavior highlights the importance of coupling a multidimensional interior ballistics (IB) code to a CSM code rather than the typical methodology of using a lumped parameter code IB code to supply a constant projectile base pressure loading (*16*).
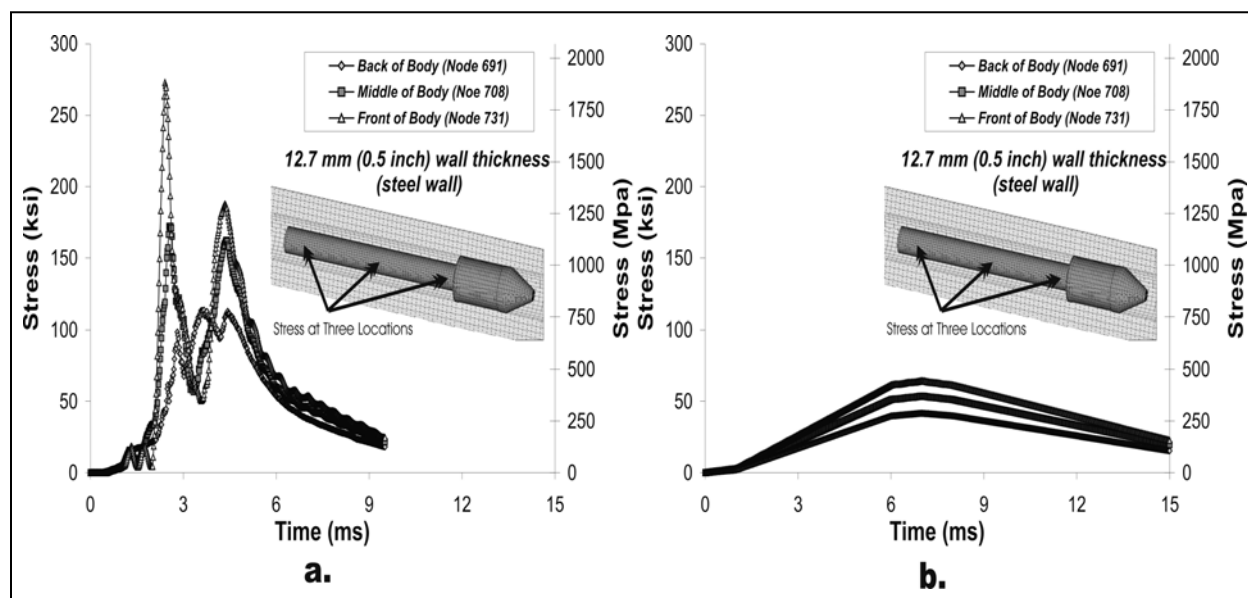
Figure 13. Effective stress results for three locations on the projectile afterbody with a 12.7-mm (0.5-in) steel body for both the propellant charge that (a) fully fills the annular region (recall figures 4–6) and (b) partially fills the annular region (recall figures 7–9).

There are a number of important observations to be gleaned from figures 12 and 13a. First, for the high-performance, dense propellant charges, the stress near the bulkhead of the projectile reaches unusually high values (figure 13a). These values would have certainly failed the steel projectile; exotic materials such as metal matrix composites may survive, but with significantly higher cost and fabrication complexity for the projectile. For this charge, the double peak in stress near the bulkhead and in the middle of the afterbody are highly atypical when compared to traditional charges in which the stress response is relatively smooth with peak stress corresponding to peak pressure loading (i.e., after significant projectile travel in the gun tube).

Figure 13b demonstrates this type of typical stress response corresponding to pressures for the modified charge shown in figures 7–9. The resulting lower stresses imply that more common materials could be used in the projectile construction.

6.   Future Efforts

The challenges now, of course, are to more fully explore the use of low-drag configurations in the annular region, including stick, strip, and scroll (wrap) propellants on both a theoretical and experimental basis. Due to current limitations of the code (i.e., resolving high loading density annular charges of these propellant types) these theoretical efforts will be published after completion of refinements to the NGEN code, ongoing both at Paul Gough Associates and ARL. Additionally, the code can be used to explore appropriate modifications to the projectile afterbody (e.g., boattailing) that have also been shown to mitigate pressure wave formation. The use of gun simulators, essential to confirmation of these and subsequent theoretical insights, are being designed and constructed at various sites including ARL (*18*).

7. References

1. Horst, A. W. Weapon System Constraints on Advances in Gun Propulsion. *5th Joint Classified Bombs/Warheads & Ballistics Symposium*, Colorado Springs, CO, 1–2 June 2002.

2. Nusca, M. J.; Horst, A. W. Progress in Multidimensional, Two-Phase Simulations of Notional Telescoped-Ammunition Solid Propelling Charge. *Proceedings of the 39th JANNAF Combustion Subcommittee Meeting*, Colorado Springs, CO, December 2003; CPIA Publication JSC CD-25.

3. Anderson, R.; Fickie, K. *IBHVG2—A User's Guide*; BRL-TR-2829; U.S. Army Ballistics Research Laboratory: Aberdeen Proving Ground, MD, July 1987.

4. Gough, P. S. *Interior Ballistics Modeling: Extensions to the XKTC Code and Analytical Studies of Pressure Gradient for Lumped Parameter Codes*; ARL-CR-460, U.S. Army Research Laboratory: Aberdeen Proving Ground, MD, February 2001.

5. Eldredge, N. RDECOM-ARDEC, Picatinny Arsenal, NJ. Private communication, 2002.

6. Gough, P. S. *Formulation of a Next-Generation Interior Ballistic Code*; ARL-CR-68; U.S. Army Research Laboratory: Aberdeen Proving Ground, MD, 1993.

7. Nusca, M. J.; Gough, P. S. *Numerical Model of Multiphase Flows Applied to Solid Propellant Combustion in Gun Systems*; AIAA paper no. 98-3695, July 1998.

8. Boris, J. P.; Landsberg, A. M.; Oran, E. S.; Gardner, J. H. *LCPFCT—A Flux-Corrected Transport Algorithm for Solving Generalized Continuity Equations*; NRL-MR/6410-93-7192, Naval Research Laboratory: Washington, DC, 16 April 1993.

9. Gough, P. S. Modeling Arbitrarily Packaged Multi-Increment Solid Propellant Charges With the NGEN Code. *Proceedings of the 33rd JANNAF Combustion Meeting*; Monterey, CA, November 1996; CPIA Publication 653, Vol. 1, pp 185–209.

10. Nusca, M. J. Application of the NGEN Code to Solid Propellant Charges of Various Propellant Configurations, *Proceedings of the 33rd JANNAF Combustion Meeting*; Monterey, CA, November 1996; CPIA Publication 653, pp 421–435.

11. Gough, P. S. Extensions to the NGEN Code: Propellant Rheology and Container Properties. *Proceedings of the 34th JANNAF Combustion Meeting*; West Palm Beach, FL, October 1997; CPIA Publication 662, Vol. 1, pp 189–205.

12. Nusca, M. J. Application of the NGEN Interior Ballistics Code to High Loading Density and 3-D Propellant Charges. *Proceedings of the 34th JANNAF Combustion Meeting*; CPIA Publication 662, Vol. 3, West Palm Beach, FL, October 1997, pp 265–281.

13. Conroy, P. J.; Nusca, M. J. Interior Ballistics Modeling of High-Loading Density Charges in a ETC Gun Using the NGEN Multiphase CFD Code, *Proceedings of the 38th JANNAF Combustion Subcommittee Meeting*; Destin, FL, April 2002; CPIA Publication 712, Vol. 2, pp 449–462.

14. Horst, A. W.; Gough, P. S. *Modeling Ignition and Flamespread Phenomena in Bagged Artillery Charges*; BRL-TR-02263; U.S. Army Ballistics Research Laboratory: Aberdeen Proving Ground, MD, September 1980.

15. Horst, A. W.; Robbins, F. W.; Gough, P. S. *A Two-Dimensional, Two-Phase Flow Simulation of Ignition, Flamespread, and Pressure-Wave Phenomena in the 155-mm Howitzer*; BRL-TR-02414; U.S. Army Ballistics Research Laboratory: Aberdeen Proving Ground, MD, July 1982.

16. Newill, J. F.; Burns, B. P.; Wilkerson, S. A. *Overview of Gun Dynamics Numerical Simulations*; ARL-TR-1760; U.S. Army Research Laboratory: Aberdeen Proving Ground, MD, September 1998.

17. Whirley, R. G.; Engelmann, B. E. *DYNA3D—A Nonlinear, Explicit, Three-Dimensional Finite Element Code for Solid and Structure Mechanics*; UCRL-MA-107254 (Rev. 1); Lawrence Livermore National Laboratory: Oak Ridge, TN, November 1993.

18. Chang, L. M. U.S. Army Research Laboratory: Aberdeen Proving Ground, MD. Private communication, October 2003.

NO. OF
COPIES   ORGANIZATION

1   DEFENSE TECHNICAL
(PDF   INFORMATION CTR
ONLY)   DTIC OCA
         8725 JOHN J KINGMAN RD
         STE 0944
         FT BELVOIR VA 22060-6218

1   COMMANDING GENERAL
          US ARMY MATERIEL CMD
          AMCRDA TF
          5001 EISENHOWER AVE
          ALEXANDRIA VA 22333-0001

1   INST FOR ADVNCD TCHNLGY
          THE UNIV OF TEXAS
          AT AUSTIN
          3925 W BRAKER LN STE 400
          AUSTIN TX 78759-5316

1   US MILITARY ACADEMY
          MATH SCI CTR EXCELLENCE
          MADN MATH
          THAYER HALL
          WEST POINT NY 10996-1786

1   DIRECTOR
          US ARMY RESEARCH LAB
          IMNE AD IM DR
          2800 POWDER MILL RD
          ADELPHI MD 20783-1197

3   DIRECTOR
          US ARMY RESEARCH LAB
          AMSRD ARL CI OK TL
          2800 POWDER MILL RD
          ADELPHI MD 20783-1197

3   DIRECTOR
          US ARMY RESEARCH LAB
          AMSRD ARL CS IS T
          2800 POWDER MILL RD
          ADELPHI MD 20783-1197

ABERDEEN PROVING GROUND

1   DIR USARL
          AMSRD ARL CI OK TP (BLDG 4600)

ABERDEEN PROVING GROUND

45   DIR USARL
     AMSRD ARL WM BA
      D LYON
      T VONG
      D HEPNER
      G BROWN
     AMSRD ARL WM BC
      M BUNDY
      G COOPER
      J DESPIRITO
      J GARNER
      B GUIDOS
      J NEWILL
      P PLOSTINS
      J SAHU
      S SILTON
      P WEINACHT
      A ZIELINSKI
     AMSRD ARL WM BD
      W ANDERSON
      R BEYER
      A BRANT
      S BUNTE
      T COFFEE
      J COLBURN
      P CONROY
      B FORCH
      A HORST
      S HOMAN
      S HOWARD
      M HURLEY
      S KARNA
      P KASTE
      A KOTLAR
      C LEVERITT
      R LIEB
      K MCNESBY
      M MCQUAID
      A MIZIOLEK
      J MORRIS
      M NUSCA (6 CPS)
      R PESCE-RODRIQUEZ
      A WILLIAMS
     AMSRD ARL WM BF
      D WILKERSON

INTENTIONALLY LEFT BLANK.